

Tenth-order lepton $g-2$: Contribution from diagrams containing a sixth-order light-by-light-scattering subdiagram internally

Tatsumi Aoyama,¹ Katsuyuki Asano,² Masashi Hayakawa,²

Toichiro Kinoshita,³ Makiko Nio,⁴ and Noriaki Watanabe²

¹*Faculty of Science, Nagoya University, Nagoya, Aichi 464-8602, Japan*

²*Department of Physics, Nagoya University, Nagoya, Aichi 464-8602, Japan*

³*Laboratory for Elementary-Particle Physics,*

Cornell University, Ithaca, New York 14853, USA

⁴*Theoretical Physics Laboratory, Nishina Center, RIKEN, Wako, 351-0198, Japan*

(Dated: July 1, 2021)

Abstract

This paper reports the result of our evaluation of the tenth-order QED correction to the lepton $g-2$ from Feynman diagrams which have sixth-order light-by-light-scattering subdiagrams, none of whose vertices couple to the external magnetic field. The gauge-invariant set of these diagrams, called Set II(e), consists of 180 vertex diagrams. In the case of the electron $g-2$ (a_e), where the light-by-light subdiagram consists of the electron loop, the contribution to a_e is found to be $-1.344\,9\,(10)\,(\alpha/\pi)^5$. The contribution of the muon loop to a_e is $-0.000\,465\,(4)\,(\alpha/\pi)^5$. The contribution of the tau-lepton loop is about two orders of magnitudes smaller than that of the muon loop and hence negligible. The sum of all of these contributions to a_e is $-1.345\,(1)\,(\alpha/\pi)^5$. We have also evaluated the contribution of Set II(e) to the muon $g-2$ (a_μ). The contribution to a_μ from the electron loop is $3.265\,(12)\,(\alpha/\pi)^5$, while the contribution of the tau-lepton loop is $-0.038\,06\,(13)\,(\alpha/\pi)^5$. The total contribution to a_μ , which is the sum of these two contributions and the mass-independent part of a_e , is $1.882\,(13)\,(\alpha/\pi)^5$.

PACS numbers: 13.40.Em, 14.60.Cd, 14.60.Ef, 12.20.Ds

I. INTRODUCTION

The anomalous magnetic moment $g - 2$ of the electron has provided the most stringent test of the validity of quantum electrodynamics, QED. The experimental value with the least uncertainty is the one obtained by the Harvard group in 2008 ($a \equiv \frac{g-2}{2}$) [1]

$$a_e(\text{HV08}) = 1\,159\,652\,180.73(28) \times 10^{-12}. \quad (1)$$

To confront the prediction of the standard model with this measurement the hadronic contribution up to the order α^3 [2–9], the electroweak contribution up to the two-loop order [10–12], and the QED radiative correction up to the eighth order must be taken into account [13–15]. In order to match or exceed further improvement in the accuracy of the experimental value, it is necessary to evaluate the tenth-order QED radiative correction to $g - 2$. To meet this challenge we launched several years ago the project to compute all 12672 Feynman diagrams that contribute to the tenth-order a_e [16, 17].

The most difficult to evaluate is the gauge-invariant set, called Set V, which consists of 6354 diagrams that have no virtual lepton loop. To deal with this set systematically we have developed an automatic code-generating algorithm `GENCODEN` [16, 18]. We now have FORTRAN codes for all diagrams of Set V generated by `GENCODEN`. Numerical evaluation of these integrals is in progress at present.

Meanwhile, we have also made steady progress in the evaluation of other types of tenth-order diagrams, and have published some of the results [17, 19, 20]. At the tenth order there appear five gauge-invariant sets of diagrams, called Set I(j), Set II(e), Set II(f), Set III(c), and Set VI(j), which contain light-by-light-scattering subdiagram(s) internally, i.e., none of whose vertices is the external vertex [16, 17]. (See Fig. 1.)

Feynman diagrams containing a light-by-light-scattering subdiagram internally appear for the first time in the eighth-order QED correction to the lepton $g - 2$. Figure 2 shows the eighth-order self-energy diagrams with the fourth-order internal light-by-light-scattering subdiagrams. Vertex diagrams relevant to lepton $g - 2$ can be obtained by inserting a single external QED vertex into one of open lepton lines labeled 1, 2, 3 of individual diagrams of Figure 2.

The diagrams of Set I(j) are those involving two fourth-order light-by-light-scattering subdiagrams, both internal, which have been evaluated and published recently [19]. The diagrams of other subsets are obtained by adding $O(\alpha)$ correction to those of Fig. 2. The

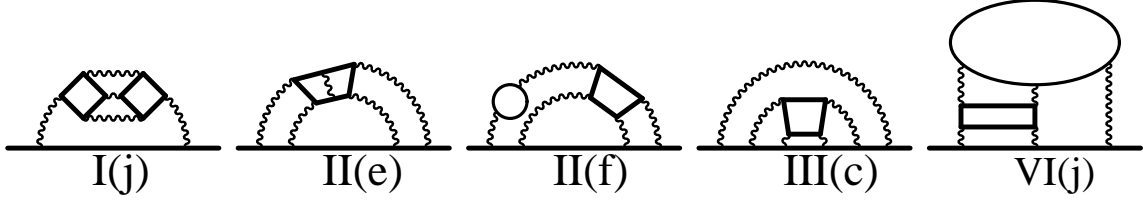


FIG. 1: Representative diagrams of gauge-invariant sets which contain an internal light-by-light-scattering subdiagram.

Set II(f) consists of diagrams obtained by inserting a second-order vacuum-polarization loop into one of internal photon lines of the diagrams of Fig. 2 in all possible ways. They have been evaluated by a simple modification of the FORTRAN codes developed previously for the eighth-order work. The result was published in Ref. [17]. The diagrams of Set III(c) are obtained by attaching a virtual photon line to the open lepton path of the individual diagrams of Fig. 2 in all possible ways. Evaluation of this set is in progress. The diagrams of Set VI(j) contain two light-by-light-scattering subdiagrams, one of which is internal, while the other is external. The numerical result of the Set VI(j) was published in Ref. [17].

The diagrams of Set II(e) are obtained by attaching both ends of a virtual photon line to the lepton loop of the individual diagrams of Fig. 2 in all possible ways, forming the sixth-order internal light-by-light-scattering subdiagram. This paper reports the result of our work on Set II(e), which consists of 180 Feynman vertex diagrams.

The paper is organized as follows. Section II describes the strategy we have adopted for the numerical study. The renormalization is set up so that ultraviolet divergences can be subtracted away without introducing spurious infrared divergence. Section III gives the results of our numerical work which covers the contributions of all diagrams of Set II(e) to a_e and a_μ . Section IV is devoted to the discussion and summary.

II. COMPUTATIONAL PROCEDURE

This section describes the strategy for computing the diagrams of Set II(e). We denote the contribution of Set II(e) to the magnetic moment of the lepton l induced by the virtual loop of lepton l' as

$$a_l(\text{II(e)}, l') = A_l(\text{II(e)}, l') \left(\frac{\alpha}{\pi} \right)^5, \quad (2)$$

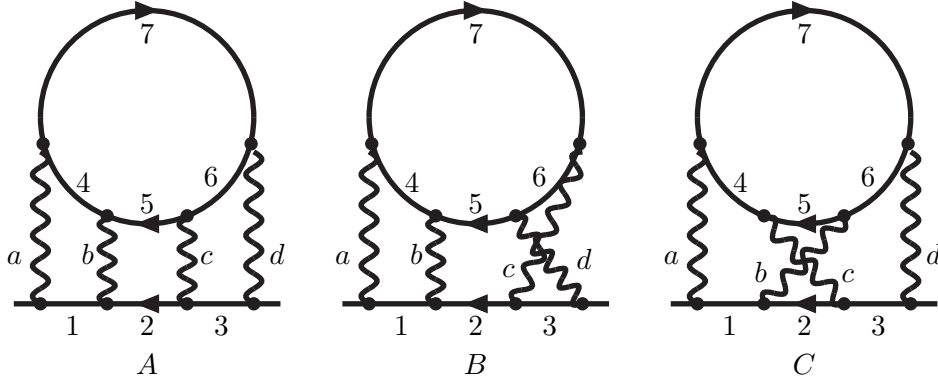


FIG. 2: Eighth-order self-energy Feynman diagrams $LL8$ that contain the fourth-order light-by-light-scattering subdiagram internally. In Ref. [27], A , B and C are called “LLJ”, “LLL” and “LLK”, respectively. The vertex diagrams are obtained by inserting a single QED vertex into one of the lepton lines 1, 2 or 3 of G ($G = A, B, C$).

where the lower case “ a ” includes the factor $(\frac{\alpha}{\pi})^5$ while the upper case “ A ” does not. Recall that $a_l(\text{II}(e), l' = l)$ and $A_l(\text{II}(e), l' = l)$ are independent of l and called mass-independent contributions. $A_l(\text{II}(e), l' \neq l)$ depends only on the mass ratio $m_{l'}/m_l$. We use the values found in Ref. [21] for lepton masses.

As explained in Sec. I, the diagrams of Set II(e) are obtained by attaching an internal photon line to the lepton loop of the individual diagrams of Fig. 2 in all possible ways. Let us denote the diagrams of Set II(e) as Gij by specifying (i) the base eighth-order diagram G , where G is one of A , B , or C of Fig. 2, and (ii) a pair (i, j) of lepton lines of the closed loop ($4 \leq i \leq j \leq 7$) to which an additional internal photon line is attached. For instance, the insertion of two QED vertices into the middle of the lines 4 and 7 of the diagram A of Fig. 2 and the introduction of a virtual photon line which connects these vertices produces the tenth-order diagram called $A47$. Representative diagrams of Set II(e) are shown in Figure 3. The charge conjugation and time reversal symmetries of QED help us to reduce the number of independent amplitudes. For instance, $A67$ gives the same contribution to $g-2$ as $A47$. Recall also that the diagram in which the lepton loop runs in the opposite direction gives the same contribution as the original one. In this way, we obtain a complete set of independent

diagrams:

$$\begin{aligned}
& A44 [4], A55 [2], A77 [2], A47 [4], A45 [4], A46 [2], A57 [2], \\
& B44 [4], B55 [4], B47 [4], B45 [4], B46 [2], B57 [2], \\
& C44 [4], C55 [2], C77 [2], C47 [4], C45 [4], C46 [2], C57 [2],
\end{aligned} \tag{3}$$

where the number in the brackets accounts for the symmetry factor for each diagram as well as the doubling due to two directions that a lepton loop takes.

Thus far no one has succeeded in evaluating the diagrams of Set II(e) analytically. We resort to the numerical means utilizing the parametric integral formulation [16, 18, 22, 23]. The evaluation of $g-2$ can be simplified significantly by focusing on the quantity associated with the self-energy diagram G_{ij} , such as the magnetic moment amplitude $M_{G_{ij}}$, using the Ward-Takahashi identity which relates the regularized self-energy function $\Sigma_{G_{ij}}(p)$ of the diagram G_{ij} to the sum $\Lambda_{G_{ij}}(p, q)$ of the contributions from the regularized vertex diagrams obtained by inserting a QED vertex into G_{ij} in all possible ways [24].

The next step is to renormalize the integrals on the computer, which we carry out by subtractive renormalization. Since the bare amplitudes of individual diagrams have different structures of UV singularities, the numerical subtraction of UV singularities must be carried out for each diagram separately. Our aim is to construct subtraction terms that (i) share the same UV singularity as the integrand of the bare amplitude in the common Feynman parameter space, and (ii) do not introduce spurious IR singularities.

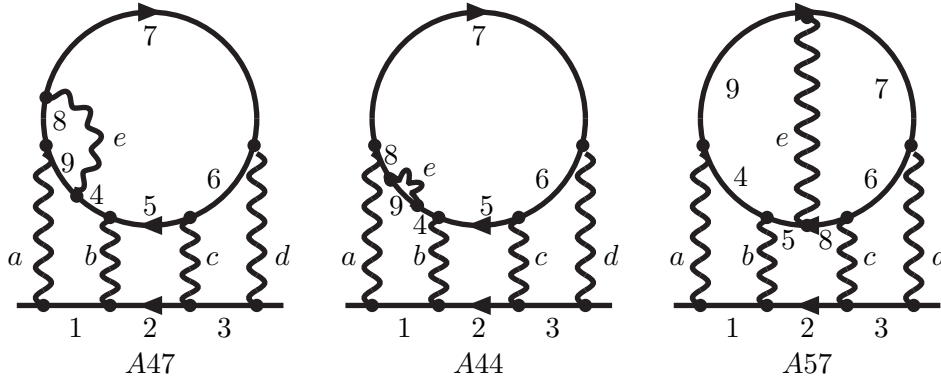


FIG. 3: Representative diagrams of Set II(e). A47 and A44 involve a second-order vertex subdiagram and a second-order self-energy subdiagram, respectively.

The second point is not a trivial requirement. For instance, the usual on-shell second-order vertex renormalization constant contains an IR divergence. In general the subtraction term constructed under the usual on-shell renormalization condition introduces an IR singularity that is not present in the bare amplitude. To avoid this problem we perform the renormalization in two steps. The first step is to construct the UV-finite amplitude ΔM_{Gij} in which only the UV-divergent part of the corresponding on-shell vertex (or self-energy) term is subtracted, leaving out the UV-finite piece unsubtracted. We call this step an *intermediate renormalization*. The second step is to carry out the finite *residual* renormalization to account for the difference between the intermediate renormalization and the usual on-shell renormalization. The IR-divergent parts of the usual on-shell renormalization constants appear in the second step but cancel out when summed over the entire gauge-invariant set.

The subtraction terms of ΔM_{Gij} are constructed as follows. The UV singularities associated with the second-order vertex and self-energy subdiagrams are subtracted via K-operation, retaining the Feynman cut-off until UV divergences cancel out by renormalization [23]. The UV singularities of the light-by-light-scattering (l - l) loops are subtracted while maintaining the Pauli-Villars regularization in order to avoid dealing with divergent hence undefined quantities. The Pauli-Villars mass is sent to infinity only after renormalization is carried out. Note that not only the usual on-shell renormalization but also the intermediate renormalization are defined on the mass-shell insofar as it is IR-safe. To avoid confusion let us call the usual on-shell renormalization as the *full renormalization* henceforth.

Let us illustrate our renormalization procedure taking A47 of Fig. 3 as an example. A47 has four UV-divergent subdiagrams which can be identified by the sets of lepton lines involved:

$$\begin{aligned} S_1 &= \{1, 2, 4, 5, 6, 7, 8, 9\}, & S_2 &= \{2, 3, 4, 5, 6, 7, 8, 9\}, \\ S_3 &= \{4, 5, 6, 7, 8, 9\}, & S_4 &= \{8, 9\}. \end{aligned} \tag{4}$$

Both subdiagrams S_1 and S_2 are the eighth-order vertex subdiagrams, S_3 is the sixth-order l - l subdiagram, and S_4 is the second-order vertex subdiagram. Each UV subtraction term of ΔM_{Gij} is associated with a Zimmermann's forest. A47 has 11 normal forests. Let C_S denote the operator which extracts the full renormalization constant of the subset S from M_{Gij} , and let K_S denote the operator which extracts the UV singularity of the subset S by the intermediate renormalization defined by the K operation, respectively. Then the UV-finite

quantity ΔM_{A47} is defined by

$$\begin{aligned}
\Delta M_{A47} = & M_{A47} - \mathbb{C}_{S_1} M_{A47} - \mathbb{C}_{S_2} M_{A47} - \mathbb{C}_{S_3} M_{A47} - \mathbb{K}_{S_4} M_{A47} \\
& + \mathbb{K}_{S_4} \mathbb{C}_{S_3} M_{A47} + \mathbb{K}_{S_4} \mathbb{C}_{S_1} M_{A47} + \mathbb{K}_{S_4} \mathbb{C}_{S_2} M_{A47} \\
& + \mathbb{C}_{S_3} \mathbb{C}_{S_1} M_{A47} + \mathbb{C}_{S_3} \mathbb{C}_{S_2} M_{A47} \\
& - \mathbb{K}_{S_4} \mathbb{C}_{S_3} \mathbb{C}_{S_1} M_{A47} - \mathbb{K}_{S_4} \mathbb{C}_{S_3} \mathbb{C}_{S_2} M_{A47}.
\end{aligned} \tag{5}$$

Expression of ΔM_{Gij} for other Gij in Eq. (3) can be written down similarly.

It is by definition that all subtraction terms on the right-hand side of Eq. (5) are factorizable. For instance, the operator \mathbb{C}_{S_1} acting on M_{A47} produces the product of L_{S_1} and M_2 :

$$\mathbb{C}_{S_1} M_{A47} = L_{S_1} M_2, \tag{6}$$

where L_{S_1} is the full eighth-order vertex renormalization constant of the diagram that contains the sixth-order light-by-light-scattering subdiagram, and $M_2 = a_2 = \frac{1}{2}$ is the second-order lepton $g-2$. Of course this equation is meaningless unless it is regularized. L_{S_1} and M_2 can be expressed as regularized integrals in the parametric integral formulation [22] on two separate Feynman parameter spaces with constraints $\sum_{i: \text{all lines} \in S_1} x_i = 1$, $\sum_{k=3, d} y_k = 1$, where y_d is the Feynman parameter associated with the photon d .

A manipulation similar to that of Sec. III D of Ref. [16] expresses $L_{S_1} M_2$ as an integral over the single Feynman parameter space with $\sum_{j \in A47} z_j = 1$. With this form of integrand of $L_{S_1} M_2$ the pointwise subtraction of the overall UV divergence of M_{A47} residing in the subdiagram S_1 can be achieved. [Actually, $\mathbb{C}_{S_1} M_{A47}$ still has divergences from the subdiagrams S_3 and S_4 which must be subtracted by other terms of Eq. (5).]

The K-operator, \mathbb{K}_{S_4} , acts on the regularized integrand $J(z)$ of M_{A47} directly and produces a function $J_{S_4}(z)$ that possesses the same UV singularity associated with the subdiagram S_4 as $J(z)$. By definition K-operation also has the factorization property. For instance, the operator \mathbb{K}_{S_4} acting on the regularized M_{A47} produces the factorized result

$$\mathbb{K}_{S_4} M_{A47} = L_2^{\text{UV}} M_{8A}, \tag{7}$$

where L_2^{UV} is the UV-divergent part of the regularized second-order on-shell vertex renormalization constant L_2 and does not include the IR-divergent part of L_2 [23]. M_{8A} denotes the amplitude of the magnetic moment from the eighth-order diagram A of Fig. 2. The

regularization mass must be sent to infinity after $\mathbf{K}_{S_4} M_{A47}$ is combined with M_{A47} . The difference of L_2^{UV} and L_2 is accounted for at the stage of the residual renormalization.

The subtraction term $\mathbf{C}_{S_3} M_{A47}$ can be written (somewhat) symbolically as

$$\mathbf{C}_{S_3} M_{A47} = \Pi(0, 0, 0, 0) M_4, \quad (8)$$

Here Π is a short-hand form of the sixth-order l - l subdiagram defined by

$$\Pi_{\kappa\lambda\mu\nu}(k_a, k_b, k_c, k_d)|_{k_a=k_b=k_c=k_d=0}, \quad (9)$$

where k_a , etc., are the momenta carried by the photon line a , etc., and M_4 is obtained from M_{A47} by shrinking the l - l loop of S_3 to a point. The UV divergence of M_{A47} arising from the subdiagram S_3 is cancelled by the term $\mathbf{C}_{S_3} M_{A47}$ of Eq. (5), which results in full renormalization of the S_3 divergence. Actually, M_{A47} contains another UV divergence arising from S_4 which we subtract by the operator \mathbf{K}_{S_4} . The complete removal of UV divergences arising from S_3 and S_4 is achieved by the combination

$$M_{A47} - \mathbf{C}_{S_3} M_{A47} - \mathbf{K}_{S_4} M_{A47} + \mathbf{K}_{S_4} \mathbf{C}_{S_3} M_{A47}. \quad (10)$$

When the contributions of all diagrams of Set II(e) listed in Eq. (3) are put together, $\Pi(0, 0, 0, 0)$ from all diagrams cancel out and we obtain a simple result

$$\begin{aligned} A_l(\text{II(e)}, l') &= \sum_{Gij \in \text{Eq. (3)}} \Delta M_{Gij} - 4 \{ (L_2 - L_2^{\text{UV}}) + (B_2 - B_2^{\text{UV}}) \} A_l(\text{LL8}, l') \\ &= \sum_{Gij \in \text{Eq. (3)}} \Delta M_{Gij} - 4 \Delta B_2 \times A_l(\text{LL8}, l'), \\ \Delta B_2 &\equiv \{ (L_2 - L_2^{\text{UV}}) + (B_2 - B_2^{\text{UV}}) \} = \frac{3}{4}. \end{aligned} \quad (11)$$

Now, at last, we can send the regulator mass to infinity. B_2 is the full second-order wave function renormalization constant and B_2^{UV} is the UV-divergent part of B_2 defined by the \mathbf{K} operation. The IR divergence of $(L_2 - L_2^{\text{UV}})$ cancels that of $(B_2 - B_2^{\text{UV}})$ leaving a finite term as expected. (Note that $B + L = 0$ while $B_2^{\text{UV}} + L_2^{\text{UV}}$ is finite but not zero. See Ref. [24] for the exact definitions of B_2^{UV} and L_2^{UV} .) Eq. (11) shows that the residual renormalization term is proportional to the eighth-order contribution $A_l(\text{LL8}, l')$ to the anomalous magnetic moment of the lepton l from the diagrams of Fig. 2, in which loops are given by lepton l' . The numerical study in Ref. [25] has provided an accurate value for the mass-independent contribution $A_e(\text{LL8}, e)$

$$A_e(\text{LL8}, e) = -0.990\,72\,(10). \quad (12)$$

In addition the paper [25] reports the electron-loop contribution to a_μ

$$A_\mu(\text{LL8}, e) = -4.432\,43\,(58). \quad (13)$$

We have also evaluated the muon loop contribution $A_e(\text{LL8}, \mu)$ to the electron $g-2$, and the tau-lepton loop contribution $A_\mu(\text{LL8}, \tau)$ to the muon $g-2$ needed for this work

$$A_e(\text{LL8}, \mu) = -0.000\,177\,8\,(12), \quad (14)$$

$$A_\mu(\text{LL8}, \tau) = -0.015\,868\,(37). \quad (15)$$

The remaining task is to evaluate every ΔM_{Gij} in various combination of the external and internal leptons.

III. NUMERICAL RESULTS OF ΔM_{Gij}

FORTTRAN codes for ΔM_{Gij} are rather complicated and not easy to obtain. In order to facilitate this problem we adapted the automating code `GENCODEN` specifically for the Set II(e) which generates the integrands of ΔM_{Gij} as FORTRAN-formatted source programs. (See Refs. [16, 18] for the details of automation.) Two independent sets of automating codes together with another set of manually-produced codes were constructed to confirm their validity.

The integral for the diagram G_{ii} , i.e, the one containing the second-order self-energy subdiagram, was found to exhibit worse convergence than the others. In order to alleviate this problem, we modify the integrand in the following way. For instance, in the diagram A_{44} in Fig. 3, which contains a second-order self-energy subdiagram, the integrand of ΔM_{Gij} depends on the Feynman parameters z_4, z_8 only through the combination $z_{48} \equiv (z_4 + z_8)$. Thus, the number of independent variables is reduced from 12 to 11. This seems to improve somewhat the convergence of iteration procedure.

The integration of ΔM_{Gij} is carried out with the help of the adaptive-iterative Monte-Carlo integration routine `VEGAS` [26] on the massively parallel computer, RIKEN Integrated Cluster of Clusters (RICC). The number of sampling points for each iteration is 10^8 for all diagrams with the second-order self-energy subdiagrams and 2×10^8 for all others.

TABLE I: Numerical results for mass-independent ΔM_{Gij} from diagrams Gij in Set II(e). Full symmetry factors are included for the individual values. The number of sampling points for each iteration is 10^8 for all diagrams with the second-order self-energy subdiagrams and 2×10^8 for all others. The first, second, third and fourth columns show the name of the diagram, the value of integrand and its uncertainty, the χ^2 value of VEGAS integration, and the number of iterations of VEGAS integration. If χ^2 is very close to 1, then the numerical integration by VEGAS is reliable.

Gij	ΔM_{Gij} (uncertainty)	χ^2	iterations
<i>A44</i>	5.397 41 (33)	1.04	2420
<i>A55</i>	2.796 88 (23)	1.09	1250
<i>A77</i>	2.422 84 (20)	1.08	1210
<i>A47</i>	0.100 26 (15)	1.02	1120
<i>A45</i>	-1.559 22 (16)	0.98	1150
<i>A46</i>	1.180 76 (12)	1.10	1140
<i>A57</i>	1.653 245 (93)	1.09	800
<i>B44</i>	-4.440 95 (34)	1.06	2660
<i>B55</i>	-4.741 06 (33)	0.99	2500
<i>B47</i>	1.725 96 (17)	1.05	990
<i>B45</i>	2.521 96 (17)	1.07	1070
<i>B46</i>	-0.349 57 (11)	1.04	1040
<i>B57</i>	-2.254 206 (97)	1.10	790
<i>C44</i>	-5.054 64 (34)	1.03	2570
<i>C55</i>	-2.398 68 (24)	1.09	1670
<i>C77</i>	-2.431 20 (22)	1.06	1460
<i>C47</i>	1.574 62 (16)	1.06	990
<i>C45</i>	1.821 84 (17)	1.00	1200
<i>C46</i>	-1.881 49 (12)	1.03	1280
<i>C57</i>	-0.401 777 (91)	1.03	710
sum	-4.317 02 (94)		

A. electron $g-2$

The results of numerical integration of ΔM_{Gij} for the mass-independent contribution to the lepton $g-2$ are presented in Table I. Following Eq. (11) the last line of Table I together with the value (12) for $A_e(\text{LL8}, e)$ yields the mass-independent contribution to $g-2$ from Set II(e) diagrams

$$A_l(\text{II}(e), l) = -1.344\ 86\ (99), \quad (16)$$

where $l = e, \mu$, or τ . Recall that the actual contribution to $g-2$, $a_e(\text{II}(e), e)$, is $A_e(\text{II}(e), e)$ times the factor $\left(\frac{\alpha}{\pi}\right)^5$.

The electron $g-2$ also receives the Set II(e) contribution induced by the virtual muon loop. To see its numerical significance, the computation of ΔM_{Gij} for the muon loop is explicitly performed. The results are shown in Table II. Putting together the last line of this table and the value (14) of $A_e(\text{LL8}, \mu)$ we obtain the muon loop contribution to the electron $g-2$ from Set II(e) diagrams

$$A_e(\text{II}(e), \mu) = -0.000\ 465\ (4). \quad (17)$$

The size of this contribution is less than the numerical uncertainty of the electron-loop contribution $A_e(\text{II}(e), e)$ given in Eq. (16). Since the tau-lepton loop contribution is expected to be about two-orders of magnitudes smaller than the muon loop contribution and hence negligible, we present the sum of Eqs. (16) and (17) as our current best value for the contribution to the electron $g-2$ from Set II(e) diagrams

$$a_e(\text{II}(e)) = -1.345\ (1) \left(\frac{\alpha}{\pi}\right)^5. \quad (18)$$

B. muon $g-2$

The main contribution of Set II(e) to the muon $g-2$ arises from the diagrams each of which is induced by an electron loop. We present the numerical result of ΔM_{Gij} for the electron-loop contribution in Table III. This table shows that the sum of ΔM_{Gij} is an order of magnitude larger than that of the mass-independent ΔM_{Gij} in Table I. However, as is seen from Eq. (13) for $A_\mu(\text{LL8}, e)$, partial cancellation takes place between the first term and the second term $[-4\Delta B_2 \times A_\mu(\text{LL8}, e)]$. As a consequence, we have

$$A_\mu(\text{II}(e), e) = 3.265\ (12). \quad (19)$$

TABLE II: Numerical results for ΔM_{Gij} of electron $g-2$ from diagrams Gij in set II(e) in each of which muon induces light-by-light scattering. Full symmetry factors are included in the individual values. The number of sampling points for each iteration is 10^8 for all diagrams with the second-order self-energy subdiagrams and 2×10^8 for all others.

Gij	ΔM_{Gij} (uncertainty) $\times 10^3$	χ^2	iterations
<i>A44</i>	11.424 89 (49)	1.19	1360
<i>A55</i>	5.822 60 (36)	1.29	640
<i>A77</i>	6.167 18 (33)	1.23	640
<i>A47</i>	3.674 56 (28)	1.06	320
<i>A45</i>	0.715 82 (275)	1.14	320
<i>A46</i>	3.296 85 (25)	1.18	400
<i>A57</i>	3.686 56 (20)	1.55	240
<i>B44</i>	-6.068 57 (45)	1.02	1280
<i>B55</i>	-7.947 942 (44)	0.98	1280
<i>B47</i>	-1.252 29 (29)	1.16	240
<i>B45</i>	0.775 54 (25)	1.04	320
<i>B46</i>	-0.389 63 (26)	0.91	240
<i>B57</i>	-3.590 13 (20)	1.54	240
<i>C44</i>	-7.361 42 (46)	1.14	1120
<i>C55</i>	-3.125 44 (31)	1.17	720
<i>C77</i>	-2.927 29 (34)	1.33	480
<i>C47</i>	0.213 13 (28)	0.95	240
<i>C45</i>	-0.306 03 (30)	0.91	240
<i>C46</i>	-3.423 30 (26)	1.29	400
<i>C57</i>	-0.383 70 (17)	1.25	240
sum	-0.998 6 (14)		

TABLE III: Numerical results for ΔM_{Gij} of muon $g-2$ from diagrams Gij in set II(e) in each of which electron induces light-by-light scattering. Full symmetry factors included in the individual values. The number of sampling points for each iteration is 10^8 for all diagrams with the second-order self-energy subdiagrams and 2×10^8 for all others.

Gij	ΔM_{Gij} (uncertainty)	χ^2	iterations
<i>A44</i>	21.914 7 (35)	1.02	2180
<i>A55</i>	10.747 4 (21)	0.99	1540
<i>A77</i>	10.438 3 (20)	0.99	1300
<i>A47</i>	6.166 8 (27)	1.01	1370
<i>A45</i>	7.843 7 (28)	1.04	1370
<i>A46</i>	-13.679 5 (14)	0.98	1050
<i>A57</i>	-14.181 8 (11)	1.09	810
<i>B44</i>	-25.919 5 (40)	1.02	3050
<i>B55</i>	-25.634 7 (37)	1.03	3050
<i>B47</i>	39.794 5 (28)	1.08	1760
<i>B45</i>	41.011 0 (28)	1.11	1810
<i>B46</i>	-16.936 4 (15)	0.99	1130
<i>B57</i>	-22.029 9 (11)	1.23	840
<i>C44</i>	-41.123 9 (42)	0.99	3010
<i>C55</i>	-20.500 5 (29)	1.02	1770
<i>C77</i>	-20.929 8 (29)	1.05	1610
<i>C47</i>	46.365 7 (30)	1.05	1810
<i>C45</i>	47.994 0 (30)	1.04	1890
<i>C46</i>	-22.236 3 (15)	1.06	1130
<i>C57</i>	-19.136 5 (12)	1.08	810
sum	-10.032 (12)		

TABLE IV: Numerical results for ΔM_{Gij} of muon $g-2$ from diagrams Gij in set II(e) in each of which tau-lepton induces light-by-light scattering. Full symmetry factors are included in the individual values. The number of sampling points for each iteration is 10^8 for all diagrams with the second-order self-energy subdiagrams and 2×10^8 for all others.

Gij	ΔM_{Gij} (uncertainty)	χ^2	iterations
<i>A44</i>	0.422 177 (18)	1.09	1600
<i>A55</i>	0.215 057 (18)	1.19	480
<i>A77</i>	0.219 086 (19)	1.18	320
<i>A47</i>	0.112 235 (14)	0.96	240
<i>A45</i>	−0.008 963 (17)	1.07	160
<i>A46</i>	0.119 699 (16)	1.37	160
<i>A57</i>	0.138 883 (10)	1.63	160
<i>B44</i>	−0.239 377 (18)	1.02	1400
<i>B55</i>	−0.298 375 (18)	0.99	1280
<i>B47</i>	−0.017 671 (16)	1.11	160
<i>B45</i>	0.053 945 (16)	1.16	160
<i>B46</i>	−0.014 195 (13)	0.96	160
<i>B57</i>	−0.140 250 5 (80)	1.43	240
<i>C44</i>	−0.288 614 (18)	1.04	1280
<i>C55</i>	−0.125 456 (18)	1.14	400
<i>C77</i>	−0.120 731 (18)	1.18	320
<i>C47</i>	0.019 880 (15)	1.13	160
<i>C45</i>	0.011 773 (16)	0.89	160
<i>C46</i>	−0.129 852 (14)	1.09	240
<i>C57</i>	−0.014 913 9 (86)	1.17	160
sum	−0.085 66 (7)		

Thus the electron-loop contribution $A_\mu(\text{II}(e), e)$ is not much larger than the muon loop contribution $A_\mu(\text{II}(e), \mu)$ of Eq. (16). Since the sign of $A_\mu(\text{II}(e), e)$ is opposite to that of $A_\mu(\text{II}(e), \mu)$, we are curious about the role that the tau-lepton contribution $A_\mu(\text{II}(e), \tau)$ might play. Table IV shows the result of ΔM_{Gij} for the Set II(e) contribution to the muon $g-2$ induced by the tau-lepton loop. Equation (11), together with the value (15) of $A_\mu(\text{LL8}, \tau)$, gives

$$A_\mu(\text{II}(e), \tau) = -0.038\,06\,(13), \quad (20)$$

which is two orders of magnitude smaller than $A_\mu(\text{II}(e), e)$ or $A_\mu(\text{II}(e), \mu)$. Summing up Eqs. (19), (16) and (20), the Set II(e) contribution to the muon $g-2$ is found to be

$$a_\mu(\text{II}(e)) = 1.882\,(13) \left(\frac{\alpha}{\pi}\right)^5. \quad (21)$$

IV. DISCUSSION AND SUMMARY

In this paper, we computed the contribution to the lepton $g-2$ from the tenth-order QED diagrams of Set II(e) that contain the sixth-order light-by-light-scattering subdiagram internally. The use of Ward-Takahashi identity, as well as the symmetries of QED, reduces the computation of 180 Feynman diagrams to that of 20 integrals ΔM_{Gij} . The intermediate renormalization to define ΔM_{Gij} is chosen so that the UV divergence associated with the second-order self-energy or vertex subdiagram is subtracted away by **K**-operation. Meanwhile the UV divergence arising from the l - l loop is subtracted by full renormalization. This leads to simplification of the final result as is seen in Eq. (11).

The Set II(e) contribution to the electron $g-2$ is obtained by evaluating the electron and muon virtual effects. The result is given in Eq. (18). The size is of the typical order of magnitude for the tenth-order. The numerical computation was carried out as accurately as possible with the available computer resources.

The contribution to the muon $g-2$ is obtained by evaluating the virtual effects of all leptons. The result is given in Eq. (21). The contribution of the electron loop to the muon $g-2$ is not much larger than the muon loop contribution.

We found that $A_\mu(\text{II}(e), e)$ in Eq. (19) involves partial cancellation between the sum of ΔM_{Gij} over all Gij in Set II(e) and the residual renormalization term in Eq. (11). In spite

of these problems we were able to obtain the result for $a_\mu(II(e))$ with the uncertainty less than 1% using the high performance computer system, RICC.

Acknowledgments

This work is supported in part by JSPS Grant-in-Aid of Scientific Research (C) Grants No. 19540322 and No. 20540261, and Grant-in-Aid of Ministry of Education Grant No. 20105002. The work of T. K. was supported by the U. S. National Science Foundation under Grant No. NSF-PHY-0757868. T. K. thanks RIKEN for the hospitality extended to him where a part of this work was carried out. Numerical computation was mostly conducted on the RIKEN Integrated Cluster of Clusters (RICC). A part of preliminary computation was also conducted on the computers of the theoretical particle physics group (E-ken), Nagoya University.

-
- [1] D. Hanneke, S. Fogwell, and G. Gabrielse, *New Measurement of the Electron Magnetic Moment and the Fine Structure Constant*, Phys. Rev. Lett. **100**, 120801 (2008) [arXiv:0801.1134 [physics.atom-ph]].
 - [2] K. Hagiwara, A. D. Martin, D. Nomura, and T. Teubner, *Improved predictions for $g-2$ of the muon and $\alpha_{\text{QED}}(M_Z^2)$* , Phys. Lett. B **649**, 173 (2007) [arXiv:hep-ph/0611102].
 - [3] F. Jegerlehner and A. Nyffeler, *The Muon $g-2$* , Phys. Rept. **477**, 1 (2009) [arXiv:0902.3360 [hep-ph]].
 - [4] M. Davier, A. Hoecker, B. Malaescu, C. Z. Yuan, and Z. Zhang, *Reevaluation of the hadronic contribution to the muon magnetic anomaly using new $e^+e^- \rightarrow \pi^+\pi^-$ cross section data from BABAR*, arXiv:0908.4300 [hep-ph].
 - [5] B. Krause, *Higher-order hadronic contributions to the anomalous magnetic moment of leptons*, Phys. Lett. B **390**, 392 (1997) [arXiv:hep-ph/9607259].
 - [6] K. Melnikov and A. Vainshtein, *Hadronic light-by-light scattering contribution to the muon anomalous magnetic moment revisited*, Phys. Rev. D **70**, 113006 (2004) [arXiv:hep-ph/0312226].
 - [7] J. Bijnens and J. Prades, *The hadronic light-by-light contribution to the muon anomaly*

- lous magnetic moment: Where do we stand ?*, Mod. Phys. Lett. A **22**, 767 (2007) [arXiv:hep-ph/0702170].
- [8] J. Prades, E. de Rafael, and A. Vainshtein, *Hadronic Light-by-Light Scattering Contribution to the Muon Anomalous Magnetic Moment*, arXiv:0901.0306 [hep-ph].
 - [9] A. Nyffeler, *Hadronic light-by-light scattering in the muon $g-2$: a new short-distance constraint on pion-exchange*, Phys. Rev. D **79**, 073012 (2009) [arXiv:0901.1172 [hep-ph]].
 - [10] A. Czarnecki, B. Krause, and W. J. Marciano, *Electroweak corrections to the muon anomalous magnetic moment*, Phys. Rev. Lett. **76**, 3267 (1996) [arXiv:hep-ph/9512369].
 - [11] M. Knecht, S. Peris, M. Perrottet, and E. De Rafael, *Electroweak hadronic contributions to $g_\mu - 2$* , JHEP **0211**, 003 (2002) [arXiv:hep-ph/0205102].
 - [12] A. Czarnecki, W. J. Marciano, and A. Vainshtein, *Refinements in electroweak contributions to the muon anomalous magnetic moment*, Phys. Rev. D **67**, 073006 (2003) [Erratum-ibid. D **73**, 119901 (2006)] [arXiv:hep-ph/0212229].
 - [13] T. Kinoshita and M. Nio, *Improved α^4 term of the electron anomalous magnetic moment*, Phys. Rev. D **73**, 013003 (2006) [arXiv:hep-ph/0507249].
 - [14] T. Aoyama, M. Hayakawa, T. Kinoshita, and M. Nio, *Revised value of the eighth-order electron $g-2$* , Phys. Rev. Lett. **99**, 110406 (2007) [arXiv:0706.3496 [hep-ph]].
 - [15] T. Aoyama, M. Hayakawa, T. Kinoshita, and M. Nio, *Revised value of the eighth-order QED contribution to the anomalous magnetic moment of the electron*, Phys. Rev. D **77**, 053012 (2008) [arXiv:0712.2607 [hep-ph]].
 - [16] T. Aoyama, M. Hayakawa, T. Kinoshita, and M. Nio, *Automated calculation scheme for α^n contributions of QED to lepton $g-2$: Generating renormalized amplitudes for diagrams without lepton loops*, Nucl. Phys. B **740**, 138 (2006) [arXiv:hep-ph/0512288].
 - [17] T. Kinoshita and M. Nio, *The tenth-order QED contribution to the lepton $g-2$: Evaluation of dominant α^5 terms of muon $g-2$* , Phys. Rev. D **73**, 053007 (2006) [arXiv:hep-ph/0512330].
 - [18] T. Aoyama, M. Hayakawa, T. Kinoshita, and M. Nio, *Automated Calculation Scheme for α^n Contributions of QED to Lepton $g-2$: New Treatment of Infrared Divergence for Diagrams without Lepton Loops*, Nucl. Phys. B **796**, 184 (2008) [arXiv:0709.1568 [hep-ph]].
 - [19] T. Aoyama, M. Hayakawa, T. Kinoshita, M. Nio, and N. Watanabe, *Eighth-Order Vacuum-Polarization Function Formed by Two Light-by-Light-Scattering Diagrams and its Contribution to the Tenth-Order Electron $g-2$* , Phys. Rev. D **78**, 053005 (2008) [arXiv:0806.3390].

- [hep-ph]].
- [20] T. Aoyama, M. Hayakawa, T. Kinoshita, and M. Nio, *Tenth-Order Lepton Anomalous Magnetic Moment – Second-Order Vertex Containing Two Vacuum Polarization Subdiagrams, One Within the Other*, Phys. Rev. D **78**, 113006 (2008) [arXiv:0810.5208 [hep-ph]].
 - [21] C. Amsler *et al.* [Particle Data Group], *Review of particle physics*, Phys. Lett. B **667**, 1 (2008).
 - [22] P. Cvitanovic and T. Kinoshita, *Feynman-Dyson rules in parametric space*, Phys. Rev. D **10**, 3978 (1974).
 - [23] P. Cvitanovic and T. Kinoshita, *New Approach To The Separation Of Ultraviolet And Infrared Divergences Of Feynman - Parametric Integrals*, Phys. Rev. D **10**, 3991 (1974).
 - [24] P. Cvitanovic and T. Kinoshita, *Sixth-order magnetic moment of the electron*, Phys. Rev. D **10**, 4007 (1974).
 - [25] T. Kinoshita and M. Nio, *Revised α^4 term of lepton $g-2$ from the Feynman diagrams containing an internal light-by-light scattering subdiagram*, Phys. Rev. Lett. **90**, 021803 (2003) [arXiv:hep-ph/0210322].
 - [26] G. P. Lepage, *A new algorithm for adaptive multi-dimensional integration*, J. Comput. Phys. **27**, 192 (1978).
 - [27] T. Kinoshita and W. B. Lindquist, *Eighth-order magnetic moment of the electron. IV. Vertex diagrams containing photon-photon scattering subdiagrams*, Phys. Rev. D **39**, 2407 (1989).